Dynamical localization and partial-barrier localization in the Paul trap

Sang Wook Kim
Nonlinear and Complex Systems Laboratory, Department of Physics, Pohang University of Science and Technology, Pohang, 790-784, Korea

Hai-Woong Lee
Department of Physics, Korea Advanced Institute of Science and Technology, Taejon, 305-338, Korea
(Received 7 September 1999; revised manuscript received 4 January 2000)

We investigate the nature of quantum localization exhibited by the center-of-mass motion of an ion in a Paul trap interacting with a standing laser field. Depending upon system parameters and the initial location of the ion, quantum suppression of chaotic diffusion is dominated by dynamical localization or localization due to partial barriers formed of broken separatrices and cantori.

PACS number(s): 05.45.Mt, 03.65.Sq, 32.80.Lg

I. INTRODUCTION

The phenomenon of quantum localization, i.e., the quantum suppression of classical diffusion, is one of the most important features of quantum dynamics and is expected to play a key role in our understanding of the issue of the quantum-classical correspondence in classically chaotic systems [1,2]. Investigations have revealed that there are two distinct quantum effects that act to suppress chaotic diffusion. One is dynamical localization, a pure quantum interference effect which is not affected by the structure of classical phase space, and the other is partial barrier localization, an effect due to partial barriers formed of broken tori (cantori) and/or broken separatrices, remnants of classical phase-space structure.

Dynamical localization in classically chaotic systems was first discovered by Casati *et al.* [3] in their investigation of the kicked rotor. The phenomenon can be understood as a dynamical version of Anderson localization in solids [4] and is thus as fundamental a phenomenon as quantum tunneling. It works in a sense opposite to quantum tunneling, because it states that there exists a part of phase space which classical dynamics allows us to explore but quantum dynamics does not. Intense theoretical and experimental investigations [5–9] that followed the numerical observation of dynamical localization by Casati *et al.* have proved convincingly that dynamical localization manifests itself also in microwave ionization of Rydberg hydrogen atoms. A recent experimental investigation [10,11] of momentum transfer in ultracold atoms interacting with a standing-wave field, in particular, has provided a direct experimental observation of dynamical localization in the periodically driven rotor system [12].

Partial barrier localization occurs because quantum and classical propagations through partial barriers formed of cantori or broken separatrices can be vastly different. Classically the partial barriers act to slow down diffusion, although they cannot completely block the flow [13]. Quantum mechanically, however, since any structure smaller than the Planck constant h is not recognized in the quantum world, the cantori or broken separatrices act as perfect barriers if the phase-space area of flux escaping through them each period of the perturbing force is smaller than h. Thus, quantum effects can suppress classical chaotic diffusion through partial barriers to the level of quantum tunneling. Partial-barrier localization is important especially when the size of the holes in the cantori or the broken separatrices is relatively small and consequently when the classical diffusion rate is small. One can thus expect a strong effect of partial-barrier localization when system parameters take on values slightly above the critical values at which the breakup of Kolmogorov-Arnol'd-Moser (KAM) tori or separatrices in the region of interest takes place.

It has been shown [14] that partial-barrier localization, especially cantori localization, can play an important role in a quantum description of a wave packet motion modeling multiphoton dissociation of a diatomic molecule. It has also been argued [15,16] that the localization seen in the numerical simulation of the kicked rotor and of the Rydberg hydrogen atom in a microwave field, attributed generally to dynamical localization, can be explained at least in part in terms of cantori inhibiting the diffusive motion. It can be suggested, for example, that the expression for the localization length found for the kicked rotor [17] in the region of small diffusion rates can be derived using the concept of cantori localization. There has even been some question [18] over whether the localization observed in the momentum transfer experiment of ultracold atoms in a standing-wave field is indeed dynamical localization. The importance of cantori localization has been emphasized in some very recent studies. For example, Borgonovi [19] has shown that dynamical localization and cantori localization can coexist in a discontinuous perturbed twist map for which the hypothesis of the KAM theorem is not satisfied. Casati and Prosen [20] have shown that the quantum motion in the stadium billiard is dominated by dynamical or cantori localization depending on the shape of the stadium. Finally, Vant *et al.* [21] reported experimental observation of cantori localization with ultracold atoms subjected to a train of double pulses.

In this paper, we report our study of quantum localization in a system which we believe exhibits partial-barrier localization due to broken separatrices and cantori as well as dynamical localization. The system is an ion in a Paul trap interacting with a standing laser field. It is the same system considered recently by Ghafar *et al.* [22]. Although Ghafar

et al. interpreted their results solely in terms of dynamical localization, a close inspection of the classical phase-space structure and associated quantum probability distributions in phase space indicates that localization due to broken separatrices and cantori cannot generally be ignored.

II. THE SYSTEM AND ITS CLASSICAL PHASE-SPACE STRUCTURE

Let us consider the center-of-mass motion of an ion in a Paul trap interacting with a standing laser field. The Hamiltonian describing the motion is given by

$$\hat{H}=\frac{1}{2m}\hat{p}^2+\frac{m\omega^2}{8}(a+2q\cos\omega\hat{t})\hat{x}^2+\frac{1}{2}\hbar\omega_a\hat{\sigma}_z + \hbar\Omega_0\hat{\sigma}_x\cos(k\hat{x}+\phi)\cos\omega_L\hat{t}, \quad (1)$$

where $\hat{p}$, $\hat{x}$, and $\hat{t}$ denote the momentum, position, and time, m is the mass of the ion, a and q denote the dc and ac voltages applied to the trap, ω is the frequency of the ac voltage, ω_L and k represent the frequency and the wave vector of the standing laser field assumed to be aligned along the x axis, ω_a is the atomic transition frequency, Ω_0 is the Rabi frequency, ϕ is the phase of the standing wave, and $\hat{\sigma}_z$ and $\hat{\sigma}_x$ are Pauli spin matrices. In order to avoid decoherence arising from spontaneous emission [23,24] and thereby focus on the issue of quantum localization, we assume that the ion is initially in its ground state and that the detuning $\Delta=\omega_L-\omega_a$ is large. Equation (1) can then be reduced, under the rotating-wave approximation, to the dimensionless form [22]

$$H=\frac{16k^2}{m\omega^2}\hat{H}=\frac{1}{2}p^2+\frac{1}{2}(a+2q\cos 2t)x^2+\Omega\cos x, \quad (2)$$

where the phase ϕ is taken to be zero, $\Omega=2\hbar k^2{\Omega_0}^2/m\omega^2\Delta$ is the effective coupling constant for the ion-laser interaction, and p, x, and t are, respectively, dimensionless momentum, position, and time defined as $p=(4k/m\omega)\hat{p}$, $x=2k\hat{x}$, and $t=\omega\hat{t}/2$. We note that, in terms of the dimensionless quantities, the Schrödinger equation reads $i\hbar_{eff}\partial\psi(x,t)/\partial t=H\psi(x,t)$ where $\hbar_{eff}=8k^2\hbar/m\omega$. Thus, the parameter $2\pi\hbar_{eff}$ is the effective Planck constant.

It has been shown [25] that the classical motion of the ion described by the Hamiltonian, Eq. (2), can be chaotic. We show in Fig. 1 the classical Poincaré surface of section for the case $a=0$, $q=0.4$, and $\Omega=0.65$, which indicates that most of the phase space is covered with a chaotic sea. The two stable islands are located around the phase points $(x=\pm\pi, p=0)$, which correspond to the minima of the standing laser field. With the ac voltage supplying the external driving force, the origin (0,0) is an unstable (hyperbolic) fixed point and its stable and unstable manifolds form homoclinic tangles. As is well known, segments of stable and unstable manifolds of hyperbolic orbits form the boundaries between regions of qualitatively different types of motion. The partial barriers formed from these segments of broken separatrices act to slow down classical diffusion from one such region to another. Quantum mechanically, however, the broken separatrices act as perfect barriers, if the phase-space area of flux escaping through the broken separatrices each period of driving force is smaller than the Planck constant h.

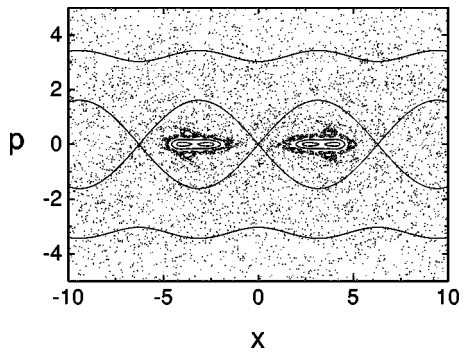

FIG. 1. Poincaré surface of section for the ion described by the Hamiltonian, Eq. (2). The dimensionless system parameters are $a=0$, $q=0.4$, and $\Omega=0.65$. The solid curves near $p\simeq\pm3.5$ correspond to the golden mean KAM tori for a system governed by the Hamiltonian (2) with $a=q=0$. The separatrices of this system are also displayed.

Figure 2 shows the stable and unstable manifolds of the hyperbolic point of our system. The phase-space area of flux through the partial barriers each period of the driving force is measured by the size of the ''turnstile'' [13] denoted by ΔW in the figure. Since the primary intersection point A in Fig. 2 maps into the point B after one period of the applied ac voltage, the phase-space area of flux through the broken separatrices during one period amounts to $2\Delta W$ ($\Delta W\simeq0.25$), and is smaller than $2\pi\hbar_{eff}$ ($=1.82$). We thus expect that the broken separatrices act as strong barriers quantum mechanically.

III. QUANTUM LOCALIZATION

Now we present results of our classical and quantum mechanical computations of the time evolution of a Gaussian wave packet which represents the ion described by the Hamiltonian of Eq. (2). For all our results reported here, $a=0$, $q=0.4$, $\Omega=0.65$, and $2\pi\hbar_{eff}=1.82$. In order to investigate quantum localization, we place the initial wave packet at a phase point in the chaotic sea. All the points in the chaotic sea are, however, not the same. From the preceding

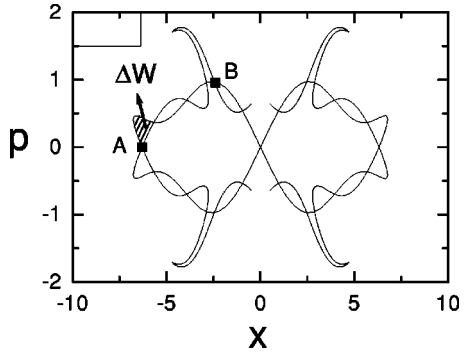

FIG. 2. Stable and unstable manifolds of the hyperbolic point (0,0). Point A is the primary homoclinic point and maps into point B after one period. ΔW represents the area of the turnstile and the box in the upper left corner shows the area of the Planck constant $2\pi\hbar_{eff}$. All parameters are the same as in Fig. 1.

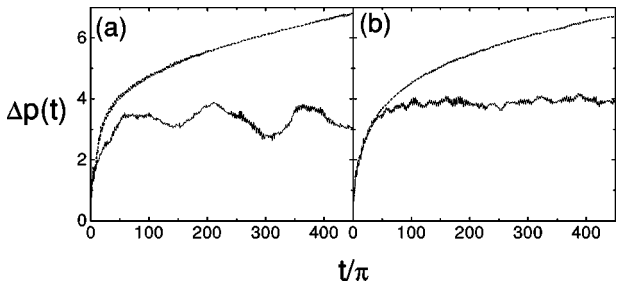

FIG. 3. Time evolution of momentum spread $\Delta p(t)$ calculated classically (upper curve) and quantum mechanically (lower curve) for the wave packet located initially at (a) (0,0) and (b) (10,0). In order to remove fast oscillations we have averaged over one period of the driving force. All parameters are the same as in Fig. 1 and $2\pi\hbar_{eff}=1.82$.

discussion, we expect the wave packet initially located along or inside the stable and unstable manifolds of the hyperbolic point to exhibit a strong effect of partial barriers formed from broken separatrices. This will be the case, for example, for a wave packet centered at the origin (0,0), for which Ghafar *et al.* [22] reported results of their calculation. On the other hand, a wave packet centered initially at (10,0), for example, will not be much affected by the partial barriers. We therefore have performed our calculations for the two positions of the initial wave packet, (0,0) and (10,0). Comparison of the result for the two different initial positions will help to distinguish the effect of dynamical localization from the effect of partial-barrier localization.

Shown in Fig. 3(a) are classical and quantum time evolutions of the momentum spread Δp of a wave packet that started its motion at (0,0). Figure 3(b) shows the same plot for the wave packet centered initially at (10,0). We clearly see quantum localization in both cases. While the classical momentum spread continues to increase with time, the quantum diffusion saturates after some time. As shown by Ghafar *et al.* [22], the classical momentum and position spreads, Δp^2 and Δx^2, of the system described by the Hamiltonian of Eq. (2) scale approximately as $t^{1/2}$. Our system therefore exhibits anomalous classical diffusion, and it is this anomalous diffusion that is suppressed in the quantum description. Despite the similarity between Figs. 3(a) and 3(b), the momentum and position distributions at large times exhibit clear differences for the two wave packets, as explained below.

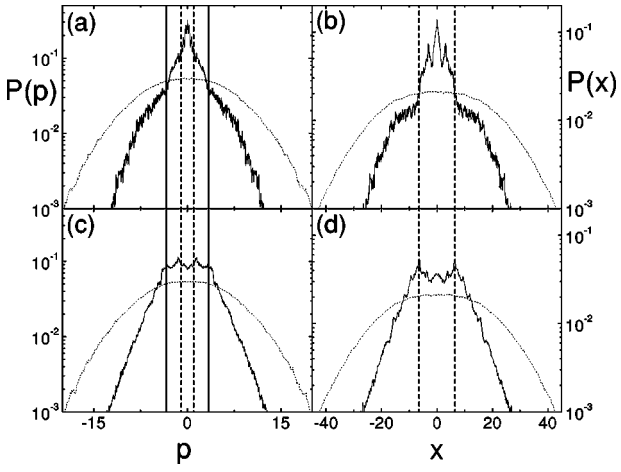

FIG. 4. Quantum (solid curve) and classical (dashed curve) distributions averaged over time in an interval $[450\pi,500\pi]$. (a) and (b) are, respectively, momentum and position distributions for the wave packet that started at (0,0), and (c) and (d) are, respectively, momentum and position distributions for the wave packet that started at (10,0). All parameters are the same as in Fig. 1 and $2\pi\hbar_{eff}=1.82$. The vertical dashed and solid lines correspond to the locations of the broken separatrices and of the golden mean KAM tori, respectively.

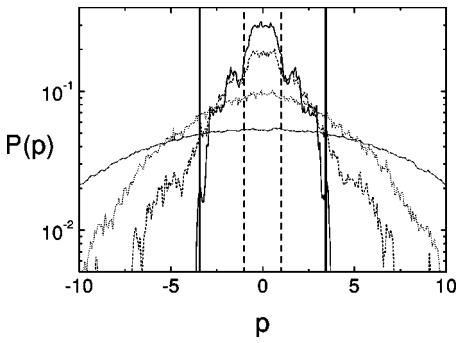

FIG. 5. Classical momentum distributions averaged over one period at $t=4\pi$ (solid curve), $t=14\pi$ (dashed curve), and $t=49\pi$ (dotted curve) for the wave packet that started at (0,0). For comparison the classical momentum distribution of Fig. 4(a) is also presented (dot-dashed curve). The vertical dashed and solid lines correspond to the locations of the broken separatrices and of the golden mean KAM tori, respectively.

We plot in Figs. 4(a) and 4(b) the momentum distribution $P(p)$ and the position distribution $P(x)$ averaged over time in an interval $[450\pi,500\pi]$ around $t=475\pi$ for the wave packet located initially at (0,0). In Figs. 4(c) and 4(d) we show the same plot for the wave packet located initially at (10,0). All four figures show that quantum distributions are narrower than the corresponding classical distributions, confirming that quantum localization takes place. Note, however, that the effects of the partial barriers formed of broken separatrices are clearly discernible in Figs. 4(a) and 4(b) with shoulders appearing on the line shape at the location of the barriers indicated by dashed vertical lines. The solid vertical lines in Fig. 4(a) indicate the positions of the golden mean KAM tori of undriven system ($q=a=0$). It appears that the remnants of these tori act to further suppress the diffusive motion which was first suppressed by the partial barriers formed of broken separatrices. As expected, the time evolution of the wave packet localized initially at (0,0) exhibits

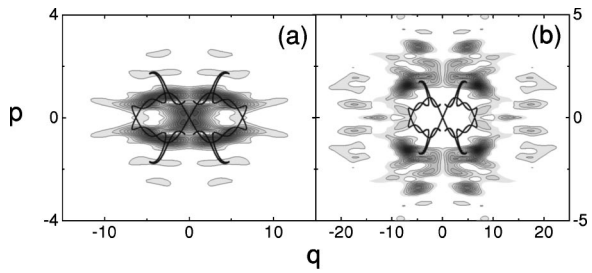

FIG. 6. Contour plot of the Husimi distribution of the wave packet at $t=450\pi$ which was initially located at (a) (0,0) and (b) (10,0). The thick curves show stable and unstable manifolds. All parameters are the same as in Fig. 1 and $2\pi\hbar_{eff}=1.82$.

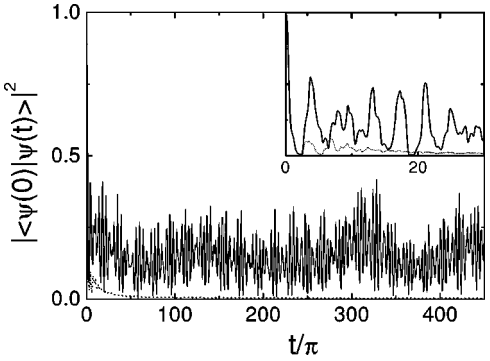

FIG. 7. Time evolution of autocorrelation calculated quantum mechanically (solid curve) and classically (dashed curve) for the wave packet which was located initially at (0,0). The inset shows an expanded view during early times. All parameters are the same as in Fig. 1 and $2\pi\hbar_{eff}=1.82$.

strong effects of the partial barriers formed from broken separatrices as well as from cantori. Similar structures in momentum distribution were also observed in a recent experimental study [21] of cantori localization. It should be noted that the localization observed here cannot be explained by the initial probability of the wave packet at (0,0) being in the two stable islands and nearby island chains, because the probability is negligibly small (less than 10^{-3}). In contrast to Figs. 4(a) and 4(b), Figs. 4(c) and 4(d) show a relatively flat region around the origin surrounded by an exponentially decreasing distribution. There is no evidence for partial barrier localization by broken separatrices here, and thus the exponential localization exhibited in Figs. 4(c) and 4(d) can be attributed to dynamical localization.

The classical distributions at the large time $t=475\pi$ shown in Fig. 4 are smooth and do not seem to indicate the presence of the partial barriers. In order to display clearly the effect of the partial barriers on classical transport, we present in Fig. 5 classical momentum distributions at earlier times. The appearance of shoulders in these distributions indicate that the partial barriers formed of cantori and of broken separatrices slow down classical propagation through them. As time becomes large, however, the shoulders disappear gradually and the distribution becomes smooth.

The role of the broken separatrices as a strong barrier to the flow can be seen more clearly from Figs. 6(a) and 6(b), where the Husimi distribution [26] of the wave packet at $t=450\pi$ are plotted for the initial wave packet positions of

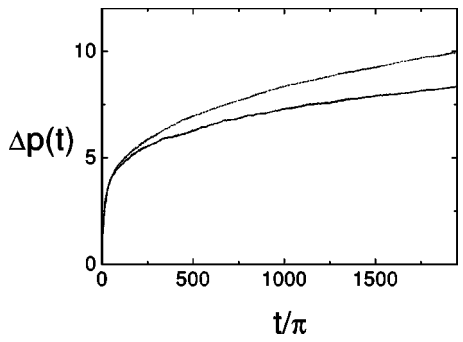

FIG. 8. Same as Fig. 3(a) except $2\pi\hbar_{eff}=0.182$.

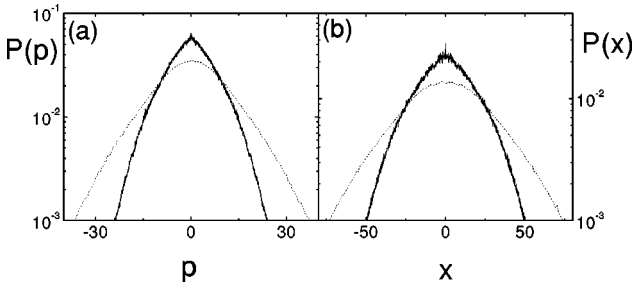

FIG. 9. Same as Figs. 4(a) and 4(b) except $2\pi\hbar_{eff}=0.182$.

(0,0) and (10.0), respectively. The two probability distributions are well separated from each other, indicating that the broken separatrices form strong barriers.

One may wonder whether the localization along the stable and unstable manifolds of the unstable fixed point seen here can be attributed to scarring [27]. We see from Fig. 7, however, that the quantum autocorrelation for the wave packet starting at (0,0) exhibits strong persistent recurrences, indicating that the localization seen here is too strong to be explained by linear scar theory [28]. Also shown in Fig. 7 is the time evolution of the classical autocorrelation function of the wave packet starting at (0,0). Since the local Lyapunov exponent at (0,0), the instability exponent of its unstable manifolds, is very large, the classical autocorrelation decay extremely rapidly. We mention here that we have also computed the quantum and classical autocorrelation functions for the wave packet starting at (10,0) and found them to decay extremely rapidly with time. That only the quantum autocorrelation for the wave packet starting at (0,0) shows a strong recurrent behavior is another indication that broken separatrices act as strong barriers.

The partial-barrier localization depends on the condition that the phase-space area of the flux through the partial barriers, i.e., the size of the turnstile, is smaller than the Planck constant h (or the effective Planck constant $2\pi\hbar_{eff}$ in our case). In order to check on this, we have repeated the calculation for the wave packet located initially at (0,0) with a new value $2\pi\hbar_{eff}=0.182$ while keeping all other parameters unchanged. The results of the calculation are displayed in Figs. 8 and 9. As expected quantum momentum and position distributions are narrower than the corresponding classical distributions and thus quantum localization still exists in this case, too. We note, however, that double-slope structure seen in Figs. 4(a) and 4(b) are totally missing in the quantum momentum and position distributions of Figs. 9(a) and 9(b). This indicates that the partial barriers formed from broken separatrices and cantori are no longer impermeable barriers quantum mechanically as well as classically. The quantum localization indicated in Figs. 8 and 9 can thus be attributed to dynamical localization.

In conclusion we have shown that the center-of-mass motion of an ion in a Paul trap interacting with a standing laser field exhibits both partial-barrier localization and dynamical localization. Which type of localization dominates depends critically upon system parameters that determine the phase-space area of the flux through the partial barriers and upon the initial location of the ion.

ACKNOWLEDGMENTS

S.W. thanks S. Tomsovic for discussions and useful comments during his visit to Harvard University. This research was supported in part by the National Science Foundation through a grant for the Institute for Theoretical Atomic and Molecular Physics at Harvard University and Smithsonian Astrophysical Observatory, and by the Agency for Defense Development (ADD) of Korea.

[1] L. E. Reichl, *The Transition to Chaos in Conservative Classical Systems: Quantum Manifestations* (Springer-Verlag, New York, 1992).

[2] *Quantum Chaos between Order and Disorder*, edited by G. Casati and B. V. Chirikov (Cambridge University Press, Cambridge, England, 1995).

[3] G. Casati, B. V. Chirikov, F. M. Izrailev, and J. Ford, in *Stochastic Behaviors in Classical and Quantum Hamiltonian Systems*, edited by G. Casati and J. Ford, Lecture Notes in Physics Vol. 93 (Springer Verlag, Berlin, 1979), p. 334.

[4] S. Fishman, D. R. Grempel, and R. E. Prange, Phys. Rev. Lett. **49**, 509 (1982).

[5] G. Casati, B. V. Chirikov, and D. L. Shepelyansky, Phys. Rev. Lett. **53**, 2525 (1984).

[6] G. Casati, B. V. Chirikov, I. Guarneri, and D. L. Shepelyansky, Phys. Rev. Lett. **59**, 2927 (1987).

[7] E. J. Galvez, B. E. Sauer, L. Moorman, P. M. Koch, and D. Richards, Phys. Rev. Lett. **61**, 2011 (1988).

[8] J. E. Bayfield, G. Casati, I. Guarneri, and D. W. Sokol, Phys. Rev. Lett. **63**, 364 (1989).

[9] M. Arndt, A. Buchleitner, R. N. Mantegna, and H. Walther, Phys. Rev. Lett. **67**, 2435 (1991).

[10] F. L. Moore, J. C. Robinson, C. F. Bharucha, P. E. Williams, and M. G. Raizen, Phys. Rev. Lett. **73**, 2974 (1994).

[11] J. C. Robinson, C. Bharucha, F. L. Moore, R. Jahnke, G. A. Georgakis, Q. Niu, and M. G. Raizen, Phys. Rev. Lett. **74**, 3963 (1995).

[12] For a theoretical analysis of the experiment, see, e.g., P. J. Bardroff, I. Bialyniki-Birula, D. S. Krähmer, G. Kurizki, E. Mayr, P. Stifter, and W. P. Schleich, Phys. Rev. Lett. **74**, 3959 (1995).

[13] R. S. Mackay, J. D. Meiss, and I. C. Percival, Physica D **13**, 55 (1984).

[14] R. C. Brown and R. E. Wyatt, Phys. Rev. Lett. **57**, 1 (1986).

[15] T. Geisel, G. Radon, and J. Rubner, Phys. Rev. Lett. **57**, 2883 (1986).

[16] R. S. Mackay and J. D. Meiss, Phys. Rev. A **37**, 4702 (1988).

[17] D. L. Shepelyansky, Physica D **28**, 103 (1987).

[18] M. Latka and B. J. West, Phys. Rev. Lett. **75**, 4202 (1995); and the resulting comments, M. G. Raizen, B. Sundaram, and Q. Niu, *ibid.* **78**, 1194 (1997); S. Meneghini, P. J. Baradroff, E. Mayr, and W. P. Schleich, *ibid.* **78**, 1195 (1997); M. Latka and B. J. West, *ibid.* **78**, 1196 (1997).

[19] F. Borgonovi, Phys. Rev. Lett. **80**, 4653 (1998).

[20] G. Casati and T. Prosen, Phys. Rev. E **59**, R2516 (1999).

[21] K. Vant, G. Ball, H. Ammann, and N. Christensen, Phys. Rev. E **59**, 2846 (1999).

[22] M. El. Ghafar, P. Törmä, V. Savichev, E. Mayr, A. Zeiler, and W. P. Schleich, Phys. Rev. Lett. **78**, 4181 (1997); M. El. Ghafar, E. Mayr, V. Savichev, P. Törmä, A. Zeiler, and W. P. Schleich, J. Mod. Opt. **44**, 1985 (1997); M. El. Ghafar, K. Riedel, P. Törmä, V. Savichev, E. Mayr, A. Zeiler, and W. P. Schleich, Acta Phys. Slov. **47**, 291 (1997).

[23] H. Ammann, R. Gray, I. Shvarchuck, and N. Christensen, Phys. Rev. Lett. **80**, 4111 (1998).

[24] B. G. Klappauf, W. H. Oskay, D. A. Steck, and M. G. Raizen, Phys. Rev. Lett. **81**, 1203 (1998).

[25] R. Chacon and J. I. Cirac, Phys. Rev. A **51**, 4900 (1995).

[26] H.-W. Lee, Phys. Rep. **259**, 147 (1995).

[27] E. J. Heller, Phys. Rev. Lett. **53**, 1515 (1984).

[28] E. J. Heller, in *Proceedings of the 1989 Les Houches Summer School*, edited by M. J. Giannoni, A. Voros, and J. Justin (Elsevier Science, Amsterdam, 1991), p. 547.